Conference on Organic Conductors and Semiconductors, Siófok, Hungary 1976

ELECTRONIC STRUCTURE AND OPTICAL PROPERTIES OF POLYSULFUR NITRIDE, $(SN)_x$

P.M. GRANT, W.E. RUDGE and I.B. ORTENBURGER

IBM Research Laboratory San Jose, California 95193, USA

ABSTRACT: We have made theoretical and experimental studies of the electronic structure and optical properties of (SN)x based on the use of OPW and pseudopotential calculational techniques and normal incidence polarized reflectance measurements. The principal finding of the calculation is the existence of a Fermi surface containing a closed direction which stabilizes (SN)x against static Peierls-Frohlich distortions thus permitting the superconducting state to occur. From the Fermi surface and band structure, we have computed the frequency-dependent dielectric tensor, $\epsilon_{\mu\nu}(\omega)$, and plasma tensor, $(\omega_p^2)_{\mu\nu}$. The calculated optical spectrum compares favorably with the results of the reflectance measurements.

Polymeric sulfur nitride, (SN)x, was first synthesized by Burt[1] in 1910, apparently as part of an effort to fix the the atomic weight of nitrogen. Over the intervening years it was recognized that (SN)x possessed an unusually high conductivity for a polymeric material. Interest quickened when it was found that for crystalline (SN)x, the conductivity had a metallic temperature dependence down to 1.2 °K and was highly anisotropic with regard to crystallographic direction.[2,3] In fact, the chain-like nature of the crystal structure[4,5] strongly suggested that (SN)x might display some of the quasi-one-dimensional characteristics of (TTF)(TCNQ) and KCP, notably the Peierls-Frohlich instability at low enough temperatures. However, it was subsequently found that (SN)x went superconducting at 0.3 °K[6] and the principal physical question thus became one of how (SN)x escaped the lattice instability usually associated with one-dimensional structures.

We decided to investigate this question by doing a thorough calculation of the one-electron properties of (SN)x. That these properties might best be represented in the Bloch representation of an OPW calculation was affirmed by the relatively large conduction bandwidths ($\sim$ 2-3 eV) inferred from specific heat[3] and optical[1,2] measurements. Furthermore, the experimental uncertainty introduced by electron-hole mean free path considerations into any k-space features to be uncovered in the calculation seemed tolerable. That is, using $\Delta k\, \ell \gtrsim 1$ as our uncertainty relation connecting direct and

reciprocal space, we find $\Delta k \lesssim$ 10% of a reciprocal lattice vector given a mean free path estimate of $\ell > 10$ Å. We feel 10 Å represents a conservative realistic lower bound on the mean free path of a carrier in an arbitrary direction in a typical (SN)x crystal. From the results of the computation and concurrent comparison with experiment, we were able to select from the following three possibilities the most likely explanation for the low temperature metallic stability of (SN)x: (1) incommensurability of the Fermi vectors with the reciprocal lattice; (2) many-body interchain effects according to the model of Klemm and Gutfreund;[7] or (3) topology of the (SN)x Fermi surface.

Details of the calculational technique, the resulting band dispersions, and comparisons with other (SN)x band structures have been presented elsewhere.[8] For our purposes, that part of the OPW band structure given in Fig. 1 will be sufficient. The directions $\Gamma\Lambda Z$ and $E \cup A$ are co-linear with the polymer chain axis (the crystallographic b-axis), the direction of highest conductivity in (SN)x, while ZE and $A\Gamma$ represent reciprocal space duals to an interchain direction. Note that the intersection of the Fermi level with bands along $\Gamma\Lambda Z$ results in two possibly incommensurate Fermi vectors in accordance with explanation (1) above. Kamimura, et al.,[9] have in fact argued that this is indeed the source of electronic stability in (SN)x. Berlinsky,[10] on the other hand, has since shown that a rigorously one-dimensional (SN)x band structure will always produce Fermi vectors

commensurate with the reciprocal lattice. From a purely empirical point of view, nature seems to "rationalize" incommensurateness in one-dimensional systems, as witnessed by the examples of (TTF)(TCNQ) and KCP where no special reason for wave vector rationality is expected and yet the Peierls-Frohlich state occurs. We believe (1) is not the answer for (SN)x. More specifically, we draw attention to the intersection of the Fermi level with bands along ZE. Intersections of this kind at other points in the Brillouin zone produce the electron-hole Fermi surfaces shown in Fig. 2. It is immediately apparent that a lowering of ground state energy through the introduction of a gap at every point on these surfaces is inconsistent with any topologically possible lattice distortion. We thus find point (3) to be the most plausible explanation for the stability of (SN)x crystals to Peierls-Frohlich effects. Nonetheless, we cannot completely rule out the mechanisms of point (2) (Ref. 7). We do feel, however, that the simplicity of point (3) and the general support of the OPW band structure properties by experiment, to be discussed next, argue effectively for our choice.

Two measureable quantities which can be directly calculated from the OPW results are the plasma tensor and the frequency dependent dielectric tensor given by the following expressions:

$$(\omega_p^2)_{\mu\nu} = 4\pi e^2 \int_{S_F} dS \, \frac{v_\mu v_\nu}{|v|}, \quad v_\mu = \frac{1}{\hbar} \frac{\partial E}{\partial k_\mu}; \quad (1)$$

$$\epsilon_{2\mu\nu}(\omega) = \frac{(\omega_p^2)_{\mu\nu}\,\tau}{\omega(1+\omega^2\tau^2)} + \frac{e^2}{\pi m^2\omega^2}\sum_{nn'}\int d^3k \times \langle nk|p_\mu|n'k\rangle\langle n'k|p_\nu|nk\rangle \times \delta(E_{n'}(k) - E_n(k) - \hbar\omega), \quad (2)$$

where the momentum matrix elements are taken with respect to the OPW Bloch functions and τ is a phenomenological Drude scattering time. The actual calculation of these quantities is effected via a pseudopotential interpolation of the OPW results followed by Gilat-Raubenheimer integration techniques. The theoretical plasma tensor, referred to its principal axes with respect to the (SN)x crystallographic coordinates, is given by Fig. 3. We see that these principal axes lie satisfyingly close to those interchain directions along which we anticipate the strongest interchain interaction to exist. The plasma tensor, in addition to determining the Drude optical properties of a metal, also determines the normal state dc conductivity and the intrinsic superconducting critical field anisotropy. It is one of the most fundamental physical properties of a metal which is directly computable from its band structure. To our knowledge, our calculation of $(\omega_p^2)_{\mu\nu}$ for (SN)x is the first for any metal. The average ratio of the b-axis component to the orthogonal components is roughly 9.5:1 which would represent the effective mass ratio for an idealized ellipsoidal Fermi surface. That these values are in reasonable agreement with experiment can be seen from Figs. 4

and 5 where we compare measured normal incidence polarized reflectivities with those calculated using Eqs. (1) and (2) along with the usual Fresnel reflectance equations. Note the close agreement between the calculated and experimental plasma reflectance minima. In computing the contribution of the Drude term in Eq. (2), we have used the experimental values of γ found by Cohen[11] and Grant, et al.[12] The Drude-like regions of the spectrum can be clearly identified; however, it is apparent that interband transitions contribute significantly to the extent of being visibly embedded in the Drude region of the R⊥b spectrum. The origin of this structure can be seen in Fig. 6 where we have plotted only the interband transition terms in ϵ_{2yy} and ϵ_{2xx}. At approximately 0.6 eV, a strong transition appears in ϵ_{2xx} which is manifested as the peak superposed on the weak Drude background of Fig. 5. We assign this structure to an M_1-type van Hove singularity arising from the parallelism of the bands intersecting the Fermi level along ZE in Fig. 1.

In the region 2-4 eV, we also observe the effects of interband transitions in both Figs. 4 and 5. Transitions between parallel bands above and below the Fermi level along ΓA are a possible source of this structure. For energies above 4 eV, we compare with the (SN)x film data of Cohen[11] reproduced in Fig. 7. These data were taken on a non-oriented film using unpolarized incident light. Various methods of averaging $\epsilon_{\mu\mu}$ were tried in an attempt to emulate experimental conditions, but the most favorable comparison occured when we simply

took half the calculated value of R∥b. This suggests that the film structure is random between polymer chains and that critical point structure from zone directions perpendicular to the chains is washed out. The observed structure most likely arises from parallel bands along DVB (not shown in Fig. 1,; see Fig. 2 of Ref. 8).

In summary, the existence of zone directions in which the Fermi surface of (SN)x closes indicates that structurally perfect (SN)x is not quasi-one-dimensional in the sense of (TTF)(TCNO) and KCP and essentially explains why Cooper pairing, and not a Peierls-Frohlich mode, is the mechanism which actually destabilizes the metallic state in the crystalline form of this material. The Fermi surface closure derives directly from band dispersion perpendicular to the polymer chain axis. From a one-electron point of view, the implications for the production of superconductivity in linear organic polymer or stacked donor-acceptor conducting systems are clear: sufficient interchain interaction must be engineered into their crystallographic structures to produce enough Fermi surface curvature to inhibit the lattice instabilities which have been the hallmark of such systems up to now.[13] That this criterion may only be marginally met in real (SN)x samples is underscored by the recent discovery of a weak Kohn anomaly at room temperature by Pintschovius and coworkers.[14] As can be seen from Fig. 2, the Fermi surface contains some fairly planar regions over much of its surface area. The effect of interchain interaction is to "pinch off" these planar regions and form separate electron-hole

volumes. Indeed, the apparent lack of long-range order in the interchain directions of (SN)x films may be connected with the failure to date to observe superconductivity in even highly oriented layers.[15] Returning to our earlier uncertainty principle argument, we note that if the mean free path in the interchain direction becomes sufficiently small (due to disorder or size effects arising from extreme fibrosity), then k-space will no longer be continuous and the carriers will not "see" the closure of the Fermi surface. Thus, gaps may begin to appear in the one-electron density of states originating either from disorder, size effects, or, if the individual chains actually become independent and isolated (hence one-dimensional), even from Peierls-Frohlich effects taking place on the microscopic scale.

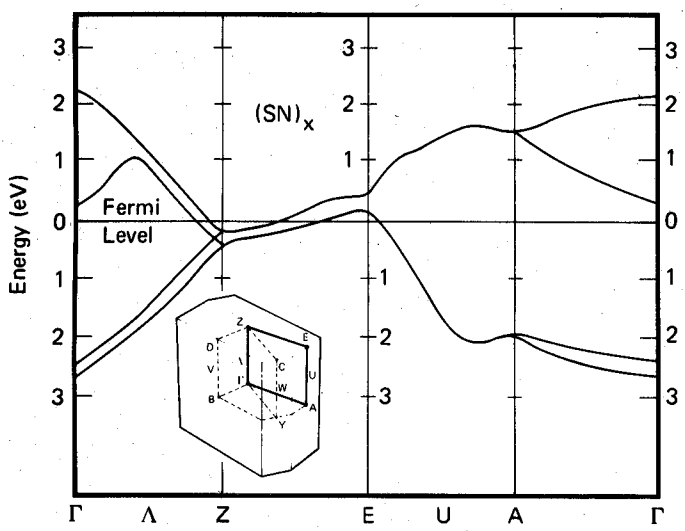

Fig. 1. Detail of the OPW band structure near E_F over the indicated path (heavy line) through the Brillouin zone.

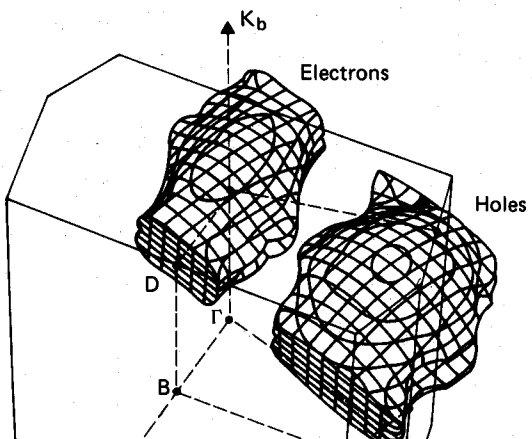

Fig. 2. The outermost electron and hole Fermi surfaces of (SN)x. Not shown is a second set of surfaces nested under those given above.

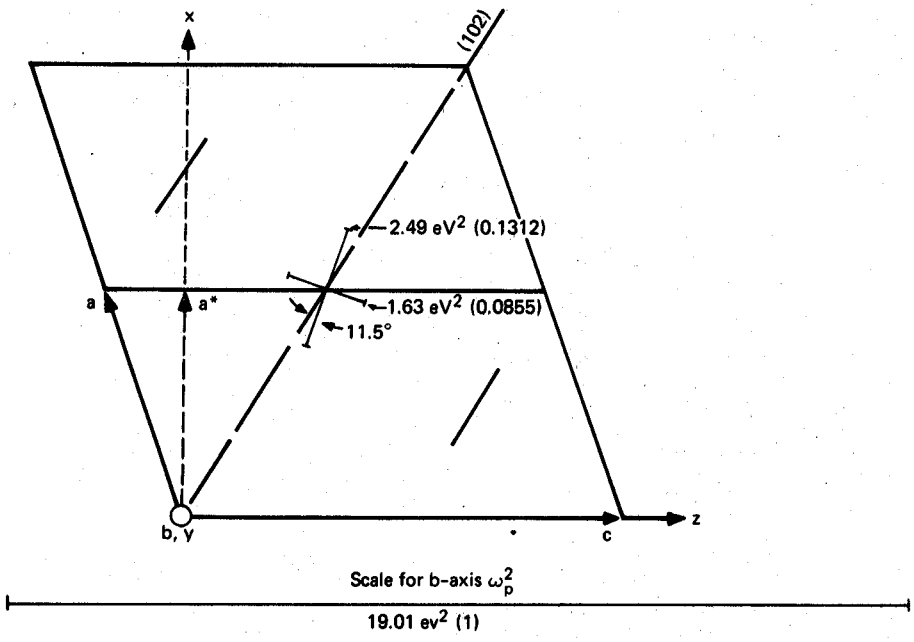

Plasma Tensor Principal Axes for Combined Holes and Electrons

Fig. 3. Principal axes of the (SN)x plasma tensor with respect to the monoclinic unit cell. The view is down the b-axis with the planes of the polymer chains indicated by the short lines in the a-b plane. The scale is set by the plasma tensor component along b with the relative ratio among components given in parentheses. The values shown are for the combined hole-electron surfaces of Fig. 1. The result $\sqrt{(\omega_p^2)_{yy}}$ = 4.4 eV is in good agreement with the measured value 4.6±1 eV from Ref. 12.

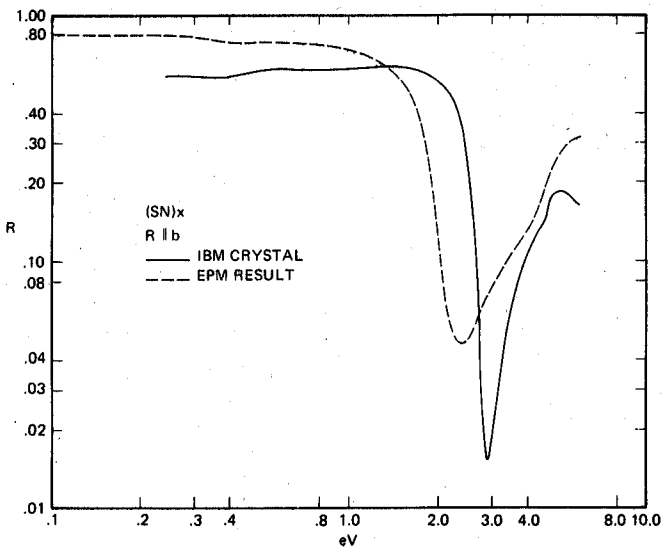

Fig. 4. Calculated and measured reflectivities for light polarized parallel to the b-axis. $\gamma_{\parallel}/\hbar$ = 1.8 eV^{-1} (Ref. 12).

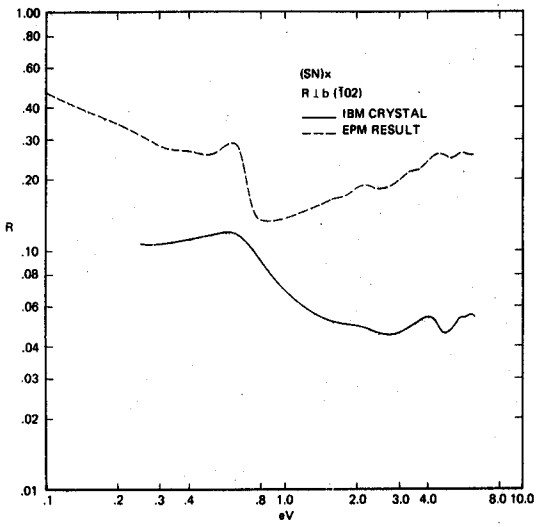

Fig. 5. Calculated and measured reflectivities for light polarized perpendicular to the b-axis and incident on the (102) plane. ϵ_{yy} was rotated to the proper frame of reference. $\gamma_{\perp}/\hbar$ = 0.6 eV^{-1} (Ref. 11) was assumed for all perpendicular directions.

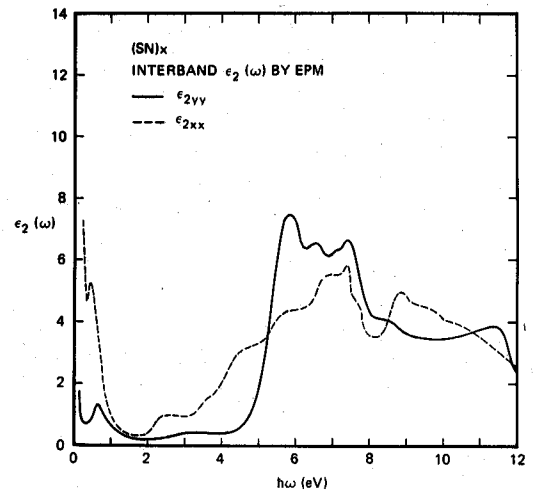

Fig. 6. Interband transition contributions to the ϵ_2 -tensor.

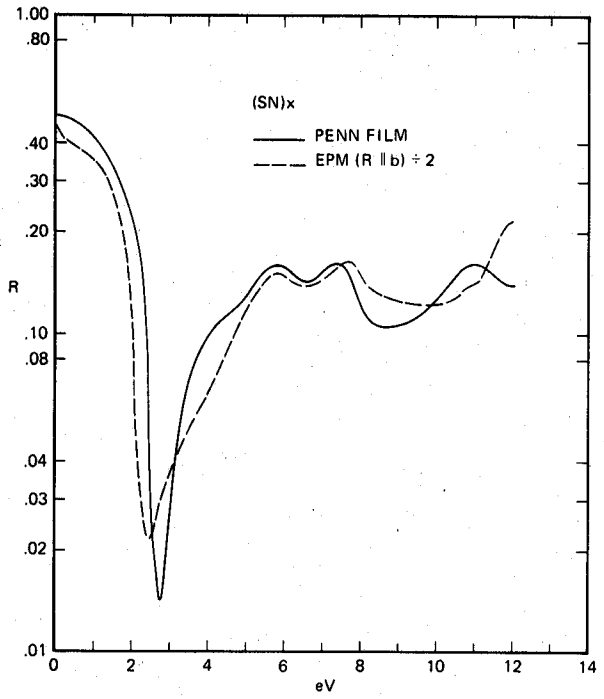

Fig. 7. Comparison between calculated and measured (SN)x unoriented film reflectivities. Film data from Cohen.[11]

REFERENCES

1. F. P. Burt, J. Chem. Soc. (London), 1171 (1910).

2. V. V. Walatka, M. M. Labes and J. H. Perlstein, Phys. Rev. Letters 31, 1139 (1973).

3. R. L. Greene, P. M. Grant and G. B. Street, Phys. Rev. Letters 34, 89 (1975).

4. M. Boudeulle, Cryst. Struct. Commun. 4, 9 (1975).

5. C. M. Mikulski, P. J. Russo, M. S. Saran, A. G. MacDiarmid, A. F. Garito and A. J. Heeger, J. Am. Chem. Soc. 97, 6358 (1975).

6. R. L. Greene, G. B. Street and L. J. Suter, Phys. Rev. Letters 34, 577 (1975).

7. R. Klemm and H. Gutfreund, to appear in Physical Review.

8. W. E. Rudge and P. M. Grant, Phys. Rev. Letters 35, 1799 (1975); W. E. Rudge, I. B. Ortenburger and P. M. Grant, (to be published in Physical Review).

9. H. Kamimura, A. J. Grant, F. Levy, A. D. Yoffe and G. D. Pitt, Solid State Commun. 17, 49 (1975).

10. A. J. Berlinsky, J. Phys. C: Solid State Phys. 9, L238 (1976).

11. M. J. Cohen, Ph.D. Thesis (University of Pennsylvania, 1975).

12. P. M. Grant, R. L. Greene and G. B. Street, Phys. Rev. Letters 35, 1743 (1975).

13. P. M. Grant, R. L. Greene, W. D. Gill, W. E. Rudge and G. B. Street, Mol. Cryst. Liq. Cryst. 32, 171 (1976).

14. L. Pintschovius, H. Wendel and H. Kahlert, Conference on Organic Conductors and Semiconductors (Hungarian Academy of Sciences, Siofok, 1976).

15. F. de la Cruz and H. J. Stolz, Solid State Commun. 20, 241 (1976); W. D. Gill, unpublished data and private communication.